SPARSE MODELS FOR DETERMINING ARTERIAL DYNAMICS

Thendral Ganesh[1], *Jayaraj Joseph*[2], *Bharath Bhikkaji*[1] *and Mohanasankar Sivaprakasam*[1,2]

[1]Indian Institute of Technology Madras, Department of Electrical Engineering, India
[2]Healthcare Technology Innovation Centre, Indian Institute of Technology Madras, India
ee12s075@ee.iitm.ac.in

ABSTRACT

This paper deals with the estimation of the inner-diameter of the Carotid Artery (CA). Arteries pulsate as blood is pumped through them by the heart. Plaque depositions along the inner wall makes the arteries rigid and obstructs the flow of blood. This increases the risk of a heart attack. The dynamics of the inner-diameter of the CA is a good indicator of this risk. An ultrasound transducer is placed on the neck of a subject and a sequence of ultrasound pulses are sent. The echoes due to the CA and other anatomical structures in the vicinity are recorded. Considering each ultrasound pulse as an input and its corresponding echo (reflections from the CA and other structures) as the output, the propagation path is modeled as a FIR filter with a sparse impulse response. Reconstruction of the echo signal, for each pulse, from the estimated impulse response significantly reduces the measurement noise. This enables the development of algorithms for accurate detection of the walls of CA and tracking of its inner-diameter dynamics. Results suggest repeatable and reliable measurements of the inner-diameter of the CA. Further more, as only the reconstructed echo signals are used, it is enough to retain the non zero filter coefficients and its corresponding indices. This leads to a large reduction in the size of the data that needs to be stored for a subject.

Index Terms— Carotid artery, Ultrasound, FIR filters, Sparsity

I. INTRODUCTION

Coronary arteries deliver oxygenated blood to the heart muscles. The accumulation of plaque (due to the deposition of lipids, calcium and other degenerative material) along the inner walls (intima) of these arteries increases their elastic stiffness and narrows their cross-sectional area. This phenomenon impedes the flow of blood and increases the blood pressure leading to a medical condition called coronary heart disease (CHD) [1]. Arterial stiffness is a significant indicator of the onset of CHD [2]. Besides blood pressure, a key parameter for determining the arterial stiffness is the diameter of the Coronary arteries [3] and [4].

Coronary arteries are not accessible for diagnosis using non-invasive techniques such as ultrasound. Recent studies have shown that hardening or stiffening of the CA is a strong indicator of the stiffening of the Coronary arteries [5]. The CA passes through the neck and supplies oxygenated blood to the head and the brain. As CA is closer to the skin, it is amenable to non-invasive diagnosis using ultrasound.

B-mode imaging systems can be used to determine the stiffness of the CA. However, B-mode imaging systems are expensive and cumbersomely large [6]. This makes it less accessible for screening a large population. In order to overcome this difficulty, an image less technology called ARTSENS was developed [7]. ARTSENS is a hand held device with a single ultrasonic transducer [8]. This transducer is configured to produce a train of ultrasound Gaussian modulated pulses, Figure 2a. When placed on the neck, close to the CA and triggered, the train of pulses get reflected by the different anatomical structures (including CA) in the neck region, Figure 1, 2b, 2c and 2d. These echoes are recorded. Anatomical structures that are static would not produce a markedly different reflection (echo) for every pulse in the train. Echoes corresponding to the CA, which pulsates due to blood pressure, would be significantly different for each pulse. Anatomical structures that are in contact with the CA would also produce different echoes for different pulses. The goal here is to distinguish the echoes due to CA from other echoes, and determine the dynamics of the inner-diameter of the CA.

In this paper, each pulse sent is considered as an input and corresponding reflected echo as the output. The propagation path (channel) is treated as the Linear Time Invariant (LTI) system (with Finite Impulse Response), Figure 3. In other words,

$$y^{(i)}(t) = u(t) \star h^{(i)}(t) + w(t), \; t = 0, 1, \cdots, N \qquad (1)$$

where $u(t)$ denotes the i^{th} Gaussian modulated sine pulse, $h^{(i)}(t)$ denotes the channel coefficients corresponding to the i^{th} pulse, $y^{(i)}(t)$ denotes the echo corresponding to the i^{th} pulse, $w(t)$ denotes the measurement noise and $\star$ denotes linear convolution. The superscript (i) is not added to the input, $u(t)$ as all Gaussian modulated sine pulses are identical. In Section 3, the details of determining $h^{(i)}(t)$ are provided. In Section 4, algorithm to determine the echoes corresponding to Proximal Wall (PW) and Distal Wall (DW) of the CA and its inner-diameter is presented. The results are presented in Section 5. The paper concludes in Section 6 with the discussion on the results.

II. SPECIFICATIONS OF THE HARDWARE

This section presents a brief description of ARTSENS. A more detailed account can be found in [7]. The key component of the ARTSENS is the ultrasound transducer (V110RM, Olympus NDT) which can both emit and record ultrasonic signals. This transducer is excited using high voltage narrow pulses of duration (t_{pw}) 20 ns, generated by Atmega - 8 microcontroller. The transducer then emits Gaussian modulated sine pulses with center frequency 5 MHz. Reflected pulses are recorded and filtered using an analog high pass Butterworth filter and amplified using a pre-amplifier (Model 5670, Panametrics NDT). The filtered signals are digitized with the sampling frequency 100 MHz using a digitizer (PXI-5152, National Instruments).

III. DATA ACQUISITION AND MODELING

As shown in Figure 2a, to capture the pulsation of the CA, a train of $M = 800$ Gaussian modulated sine pulses was generated. Here each pulse is of width 20 ns and the time between two pulses is 10 ms (t_{pr}). The echoes corresponding to all the 800 pulses were recorded [9]. Plots of the echoes corresponding to $M = 10, 150$ and 250 are presented in Figures 2b, 2c and 2d respectively. These figures show three significant echoes, from which any two adjacent echoes could be from the walls of the CA. Figure 1 shows the cross-section of the CA and its layers. The echoes from the PW (marked as 1 and 2 in Figure 1) and the echoes from the DW (marked as 3 and 4 in Figure 1) could be either first and second or second and third significant echoes in the Figures 2b, 2c and 2d respectively. This will be determined in the following.

Equation (1) can be re-written as,

$$y^{(i)} = Uh^{(i)} + w^{(i)}, i = 1, 2, \cdots, M \tag{2}$$

where, $y^{(i)} = [y^{(i)}(0), y^{(i)}(1), \cdots, y^{(i)}(N)]^T$, $h^{(i)} = [h^{(i)}(0), h^{(i)}(1), \cdots, h^{(i)}(N)]^T$, $w^{(i)}$ denotes the noise vector, (i) denotes the i^{th} pulse.

U is the $N \times N$ convolution matrix,

$$U = \begin{bmatrix} u(1) & 0 & 0 & \cdots & 0 \\ u(2) & u(1) & 0 & \cdots & 0 \\ \vdots & \vdots & \vdots & \vdots & \vdots \\ u(N) & \cdots & \cdots & u(2) & u(1) \end{bmatrix}_{N\times N}$$

As there are only a few significant reflections, $h^{(i)}$ is considered to be a sparse vector. Therefore, as in [10], $h^{(i)}$ is chosen to be

$$\arg\min_h \beta \left\|y^{(i)} - Uh^{(i)}\right\|_2 + \lambda \left\|h^{(i)}\right\|_1, \tag{3}$$

where $\left\|h^{(i)}\right\|_1$ denotes the l_1 norm, $\|\cdot\|_2$ denotes the l_2 norm and λ is the regularization parameter. The values of β and γ were fixed as 4 and 9 respectively to get the required results.

Once the sparse channel coefficient $h^{(i)}$ is obtained, the denoised signal $y_d^{(i)}$ of i^{th} pulse is reconstructed by,

$$y_d^{(i)} = Uh^{(i)} \tag{4}$$

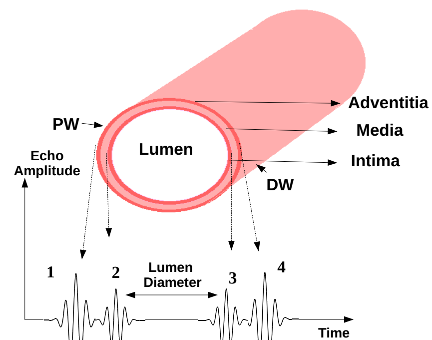

Fig. 1: Cross section of CA and echoes from its layers

Figure 4a shows the sparse channel coefficient $h^{(1)}$ and Figure 4b shows reconstructed signal $y_d^{(1)}$.

IV. ALGORITHM TO LOCATE ARTERY WALLS

In this section, algorithms to detect the walls and to track the inner-diameter of the CA are presented.

The reconstructed signal $y_d^{(i)}$ is obtained for all $i = 1, 2, \cdots, 800$. A binary signal,

$$b^{(i)} = \begin{cases} 1, & y_d^{(i)}(n) \geq \max(y_d^{(i)})/100 \\ 0, & \text{otherwise} \end{cases}, i = 1, 2, \cdots, 800$$

is generated by thresholding each $y_d^{(i)}$.

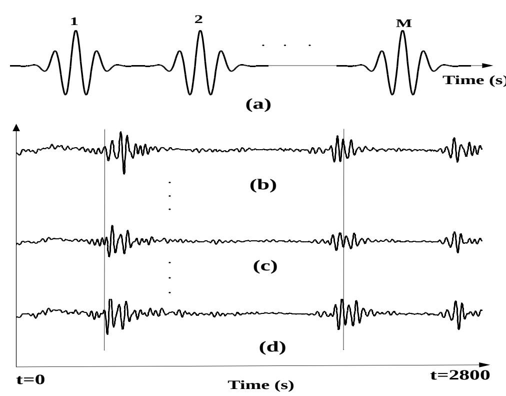

Fig. 2: (a) Train of M Gaussian modulated sine pulses (b) Reflected pulse for M = 10 (c) Reflected pulse for M = 150 (d) Reflected pulse for M = 250

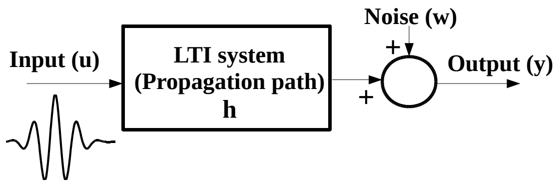

Fig. 3: Propagation path as a LTI system

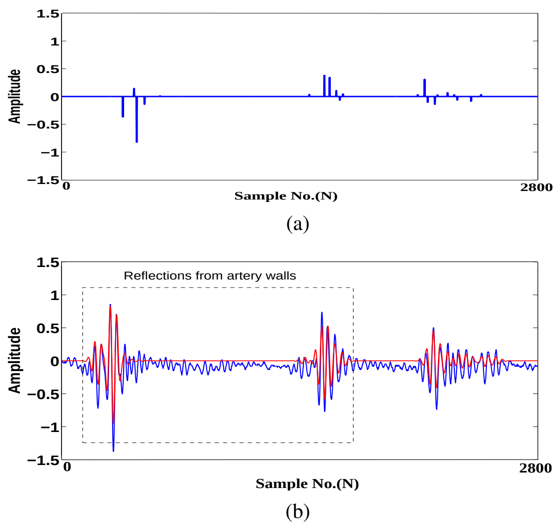

Fig. 4: (a) Sparse channel coefficient $h^{(1)}$ (b) The echo from CA (blue) and Reconstructed signal $y_d^{(1)}$ (red)

Using the binary signals $b^{(i)}$, a matrix,

$$D = [b^{(1)}(n)\ b^{(2)}(n)\ \cdots\ b^{(800)}(n)]^T \tag{5}$$

is formed.

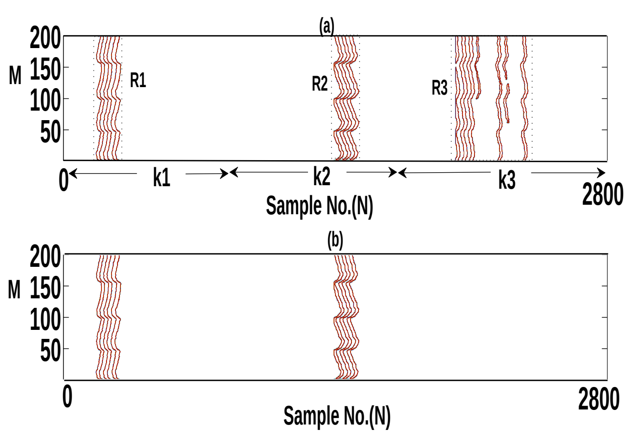

Fig. 5: (a) Contour plot of the binary matrix D that shows the pulsating motion of the CA. (b) Contour plot of the binary matrix D after detecting the walls of the artery.

Figure 5a shows the contour plot of the binary matrix D with y-axis denoting the row indices and x-axis denoting the column indices. The blank space represents the zero values and the colored represents the ones in the matrix. The pulsating motion of CA is apparent from this plot. It could also be noted from the Figure 5a that the first two colored blocks R_1 and R_2 move in opposite directions while R_3 moves in the same direction as R_2. As CA expands (diastole) and contracts (systole), in a cardiac cycle, its walls move in opposite direction. This suggests R_1 and R_2 corresponds to the walls of CA. The following algorithm detects the walls of CA.

Note that each blocks are separated by large number of zeros (> 100). Hence matrix D can be distinctly broken into blocks as,

$$D_{800\times N} = [B_1|\,B_2|\,B_3] \tag{6}$$

where B_1, B_2 and B_3 are $800\times k_1$,$800\times k_2$ and $800\times k_3$ matrices respectively and $k_1+k_2+k_3 = N$. Here $k_1 = 600$, $k_2 = 600$ and $k_3 = 1600$. Let

$$s_m^{(B_p)} = \underset{\substack{x \\ B_p(m,x)=1}}{\arg\min}\{x\} + \sum_{j=0}^{p-1} k_j\ ,\ p = 1,2,3 \tag{7}$$

$$e_m^{(B_p)} = \underset{\substack{x \\ B_p(m,x)=1}}{\arg\max}\{x\} + \sum_{j=0}^{p-1} k_j\ ,\ p = 1,2,3 \tag{8}$$

where $k_0 = 0$. Here $s_m^{(B_p)}$ and $e_m^{(B_p)}$ are the indices when one appears for the first and last time in the m^{th} row of B_p respectively.

Using (7) and (8), a 800×6 matrix X is constructed with its m^{th} row being,

$$X_m = \left[s_m^{(B_1)}\quad e_m^{(B_1)}\quad s_m^{(B_2)}\quad e_m^{(B_2)}\quad s_m^{(B_3)}\quad e_m^{(B_3)}\right] \tag{9}$$

for $m = 1,\ 2\cdots,\ 800$.

To identify the walls of artery, minimum 2 rows of the matrix X are required. Consider $F(< 20)$ rows of matrix X. In order to determine the direction in which the ones across the rows move in the block B_1, define the sets $Q = \{s_1^{(B_1)},\ s_2^{(B_1)}, \cdots s_F^{(B_1)}\}$,

$$R = \begin{cases} \{s_1^{(B_1)}, s_1^{(B_1)}+1, \cdots, s_F^{(B_1)}-1, s_F^{(B_1)}\}, & s_1^{(B_1)} < s_F^{(B_1)} \\ \{s_F^{(B_1)}, s_F^{(B_1)}+1, \cdots, s_1^{(B_1)}-1, s_1^{(B_1)}\}, & s_1^{(B_1)} > s_F^{(B_1)} \end{cases}$$

and $S = \{s_2^{(B_1)},\ s_3^{(B_1)}, \cdots s_{F-1}^{(B_1)}\}$. If $\tilde{S} = \{s_i^{(B_1)} \in S\,|\,s_i^{(B_1)} \notin R\} = \phi$ then

$$\text{direction} = \begin{cases} \text{L}, & s_1^{(B_1)} - s_F^{(B_1)} > 0 \\ \text{R}, & s_1^{(B_1)} - s_F^{(B_1)} < 0 \end{cases}. \tag{10}$$

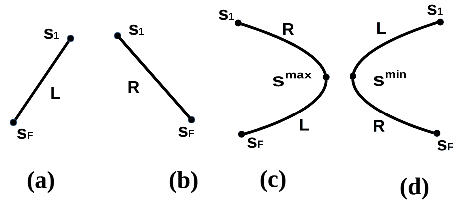

Fig. 6: All possible directions

This case refers to the block of ones moving in Figures 6a and 6b. If $\tilde{S} = \{s_i \in S \,|s_i \notin R\} \neq \phi$, define

$$s^{max} \quad = \quad \max\left\{ s_i^{(B_1)} \in \tilde{S}|\, s_i^{(B_1)} > s_1^{(B_1)} \right\}$$

and

$$s^{min} \quad = \quad \min\left\{ s_i^{(B_1)} \in \tilde{S}|\, s_i^{(B_1)} < s_1^{(B_1)} \right\}$$

The direction is given by,

$$\text{direction} = \begin{cases} \text{R} \rightarrow \text{L}, & s^{max} > s_1^{(B_1)},\, s^{min} > s_1^{(B_1)} \\ \text{L} \rightarrow \text{R}, & s^{max} < s_1^{(B_1)},\, s^{min} < s_1^{(B_1)} \end{cases}.$$

This case refers to the Figures 6c and 6d.

This procedure is repeated for blocks B_2 and B_3. Once the direction is found in each block, find the two consecutive blocks having opposite directions. Here B_1 and B_2 have opposite direction and thus these blocks corresponds to the walls of the artery. Block B_3 can be removed.

An estimate of the inner diameter of CA is,

$$L_d = \left[(s_1^{(B_2)} - e_1^{(B_1)})c/2f_s \quad \cdots \quad (s_M^{(B_2)} - e_M^{(B_1)})c/2f_s \right]^T$$

where $c = 1540m/s$ speed of sound in tissues and $f_s = 100\,MHz$ is the sampling frequency.

Figure 7 shows the plot inner diameter. Note that the repeatability is exceptionally good with precision of $\pm 0.5\%$.

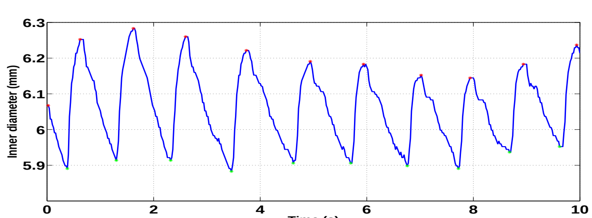

Fig. 7: Inner diameter

V. RESULTS

Ultrasound data from 30 human volunteers were collected using ARTSENS. For each human volunteer echoes of 800 (M=800) pulses were recorded. Here each echo is referred to as a frame. Out of the 800 frames, F (< 20) frames were used to detect the walls of CA. To estimate the performance of the wall detection algorithm, a parameter known as Hit Rate (HR) was calculated. If the algorithm detects the PW and DW of the artery then it is called a hit. For each volunteer,

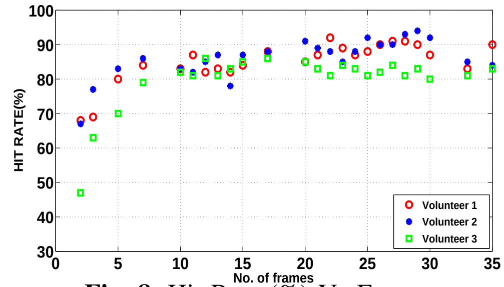

Fig. 8: Hit Rate (%) Vs Frames

F (< 20) consecutive frames of the 800 frames were picked. The choice of F consecutive frames being random. This process was repeated for nearly 100 times for each volunteer and for different number of frames F. The HR was calculated as

$$\text{HR} = \frac{\text{No.of Hits}}{\text{No.of Trials}} \times 100 \qquad (11)$$

The plot of Hit rate Vs different number of frames (F) is shown in Figure 8. The algorithm could find the artery walls more than 80% of the times when F ($\geq$5) were used.

VI. CONCLUSION

In this paper, the problem of detection of walls of CA and the estimation of its inner diameter was considered. A train of Gaussian modulated sine pulses are sent and echoes due to CA and other anatomical structures were recorded. Echoes (frames) due to each pulse was considered as an output of a FIR filter with a sparse impulse response. Signals reconstructed using these sparse filter coefficients and the input pulse were used for detecting the walls and estimating the inner diameter of CA. An algorithm to detect walls of CA was tested to give Hit Rate greater than 80% when more than five frames were used. The estimated inner diameter of CA was repeatable and reliable.

Note, it is enough to store the non-zero filter coefficients and its corresponding indices as opposed to storing the entire data. In most cases, it was found that number of non- zero filter coefficients was less than 25 while the length of an echo was 2800. This brings the large reduction in the data size, which is significant when storing data for a large population.

VII. REFERENCES

[1] http://www.britannica.com/EBchecked/topic/138261/coronary-heart-disease.

[2] J. Blacher, R. Asmar, S. Djane, G. M. London, and M. E. Safar, “Aortic pulse wave velocity as a marker of cardiovascular risk in hypertensive patients,” *Hypertension*, vol. 33, no. 5, pp. 1111–1117, 1999.

[3] J. J. Oliver and D. J. Webb, “Noninvasive assessment of arterial stiffness and risk of atherosclerotic events,” *Arteriosclerosis, Thrombosis, and Vascular Biology*, vol. 23, no. 4, pp. 554–566, 2003.

[4] M. Cecelja and P. Chowienczyk, “Role of arterial stiffness in cardiovascular disease,” *JRSM cardiovascular disease*, vol. 1, no. 4, p. 11, 2012.

[5] D. Baldassarre, A. Hamsten, F. Veglia, U. de Faire, S. E. Humphries, A. J. Smit, P. Giral, S. Kurl, R. Rauramaa, E. Mannarino *et al.*, “Measurements of carotid intima-media thickness and of interadventitia common carotid diameter improve prediction of cardiovascular events: results of the improve (carotid intima media thickness [imt] and imt-progression as predictors of vascular events in a high risk european population) study,” *Journal of the American College of Cardiology*, vol. 60, no. 16, pp. 1489–1499, 2012.

[6] D. E. Ilea, C. Duffy, L. Kavanagh, A. Stanton, and P. F. Whelan, “Fully automated segmentation and tracking of the intima media thickness in ultrasound video sequences of the common carotid artery,” *Ultrasonics, Ferroelectrics and Frequency Control, IEEE Transactions on*, vol. 60, no. 1, 2013.

[7] J. Joseph and V. Jayashankar, “A virtual instrument for automated measurement of arterial compliance,” *Journal of Medical Devices*, vol. 4, no. 4, p. 045004, 2010.

[8] http://www.htic.iitm.ac.in/?q=artsens.

[9] J. Joseph, J. Venkataraman, V. J. Kumar, and S. Suresh, “Non-invasive estimation of arterial compliance,” in *Instrumentation and Measurement Technology Conference (I2MTC), 2011 IEEE*. IEEE, 2011, pp. 1–5.

[10] F. Santosa and W. W. Symes, “Linear inversion of band-limited reflection seismograms,” *SIAM Journal on Scientific and Statistical Computing*, vol. 7, no. 4, pp. 1307–1330, 1986.